ISPRS Journal of Photogrammetry and Remote Sensing 91 (2014) 98–113

Contents lists available at ScienceDirect

ISPRS Journal of Photogrammetry and Remote Sensing

journal homepage: www.elsevier.com/locate/isprsjprs

Mapping seasonal rice cropland extent and area in the high cropping intensity environment of Bangladesh using MODIS 500 m data for the year 2010

Murali Krishna Gumma [a,b], Prasad S. Thenkabail [c], Aileen Maunahan [a], Saidul Islam [a,d], Andrew Nelson [a,*]

[a] International Rice Research Institute, Los Baños, Philippines
[b] International Crops Research Institute for the Semi-Arid Tropics, Patancheru 502324, India
[c] U.S. Geological Survey (USGS), Western Geographic Science Center, Flagstaff, AZ 86001, United States
[d] Bangladesh Rice Research Institute, Gazipur 1701, Bangladesh

ARTICLE INFO

Article history:
Received 15 February 2012
Received in revised form 11 February 2014
Accepted 18 February 2014

Keywords:
Seasonal rice mapping
MODIS NDVI
Cropping intensity
Spectral matching techniques
Field-plot information
Bangladesh

ABSTRACT

Rice is the most consumed staple food in the world and a key crop for food security. Much of the world's rice is produced and consumed in Asia where cropping intensity is often greater than 100% (more than one crop per year), yet this intensity is not sufficiently represented in many land use products. Agricultural practices and investments vary by season due to the different challenges faced, such as drought, salinity, or flooding, and the different requirements such as varietal choice, water source, inputs, and crop establishment methods. Thus, spatial and temporal information on the seasonal extent of rice is an important input to decision making related to increased agricultural productivity and the sustainable use of limited natural resources. The goal of this study was to demonstrate that hyper temporal moderate-resolution imaging spectroradiometer (MODIS) data can be used to map the spatial distribution of the seasonal rice crop extent and area. The study was conducted in Bangladesh where rice can be cropped once, twice, or three times a year.

MODIS normalized difference vegetation index (NDVI) maximum value composite (MVC) data at 500 m resolution along with seasonal field-plot information from year 2010 were used to map rice crop extent and area for three seasons, *boro* (December/January–April), *aus* (April/May–June/July), and *aman* (July/August–November/December), in Bangladesh. A subset of the field-plot information was used to assess the pixel-level accuracy of the MODIS-derived rice area. Seasonal district-level rice area statistics were used to assess the accuracy of the rice area estimates. When compared to field-plot data, the maps of rice versus non-rice exceeded 90% accuracy in all three seasons and the accuracy of the five rice classes varied from 78% to 90% across the three seasons. On average, the MODIS-derived rice area estimates were 6% higher than the sub-national statistics during *boro*, 7% higher during *aus*, and 3% higher during the *aman* season. The MODIS-derived sub-national areas explained (R^2 values) 96%, 93%, and 96% of the variability at the district level for *boro*, *aus*, and *aman* seasons, respectively.

The results demonstrated that the methods we applied for analysing and interpreting moderate spatial and high temporal resolution imagery can accurately capture the seasonal variability in rice crop extent and area. We discuss the robustness of the approach and highlight issues that must be addressed before similar methods are used across other areas of Asia where a mix of rainfed, irrigated, or supplemental irrigation permits single, double, and triple cropping in a single calendar year.

* Corresponding author. Address: International Rice Research Institute (IRRI), DAPO Box 7777, Metro Manila, Los Baños, Philippines. Tel.: +63 (2) 580 5600x2627; fax: +63 (2) 580 5699.
E-mail addresses: m.gumma@cgiar.org (M.K. Gumma), a.nelson@irri.org (A. Nelson).

http://dx.doi.org/10.1016/j.isprsjprs.2014.02.007
0924-2716/

1. Introduction

1.1. Background

Agriculture in Bangladesh is an important sector in the economy: it contributed about 20% of the gross domestic product (GDP) in 2010 and employs 63% of the country's population (BBS, 2010). Rice is the most important crop within the sector 58.1%, of the total geographic area was covered by rice averaged across 2008–12 (FAO, 2013), especially in terms of livelihood, providing food, employment, and income for much of the rural population. The person–land ratio on cropland has increased by 42–43% in only the last two decades (Asaduzzaman et al., 2010). The pressure to convert agricultural land to other uses and the increase in the human population from 138 million in 2000 to 254.6 million in 2050 (Cohen, 2004) means that productivity per unit area must increase by 97.4% (Idso, 2011) to meet this demand. This productivity gain can be achieved through a combination of higher yields per crop (better management or improved varieties), a reduction in losses (such as post-harvest losses) and higher crop intensification (the cultivation of more than one crop per year in the same location). Here we focus on cropping intensity as one approach to increase production sustainably in a well-managed cropping system (Biggs et al., 2006; Frolking et al., 2006).

Seasonal maps of the cropped area could be combined with other information on environmental and social factors to pinpoint areas where productivity could be increased. Furthermore, they could identify areas where second or third seasons could be considered. One example could be the development of new cropping calendars that mitigate the risk of exposure to coastal salinity intrusion, flooding, or drought. Another example could be the introduction of shorter duration varieties allowing time for an additional crop or varieties that can better tolerate biotic and abiotic stresses thus opening up land in seasons that were otherwise left fallow. The premise in producing this type of spatial information by season is to identify areas for intensification and to suggest development pathways towards increasing production sustainably. One such region is Rajshahi in Bangladesh, where cropping intensity is limited to 115% because of restricted irrigation potential (Allard et al., 2005). Information on cropped area often comes from nationally mandated agencies but may not fulfill the requirements for identifying opportunities to sustainably increase production through higher intensity.

Statistical data on crop area collected by agricultural ministries provide an overview of crop areas at varying levels of spatial and temporal detail (Gaur et al., 2008; Gumma et al., 2011a). Sometimes these data are available only for the entire nation (level 0 detail) but more are usually reported at state (level 1) or district (level 2) granularity. Seasonal data for countries with more than one cropping season are usually even more restricted in their availability and such aggregate data cannot be easily combined to estimate cropping intensity. The spatial and temporal detail in statistical data are insufficient for targeted policy making and there is a need for other approaches such as validated maps derived from remote sensing to deliver relevant and timely layers of information for seasonal land use and resource planning. We argue that an assessment of current cropping intensity is a first step towards providing spatial information on intensification options and that current information sources do not capture this sufficiently. Remote sensing is one approach to fill this information gap.

1.2. Examples of remote-sensing approaches for rice mapping

Remote sensing has been demonstrated to provide an alternative, quick, and independent approach for the estimation of cropping intensity, area, and changes in a country (Badhwar, 1984; Lobell et al., 2003; Thenkabail, 2010; Thenkabail et al., 2009; Thiruvengadachari and Sakthivadivel, 1997). Several studies have reported the use of multi-spectral and multi-temporal data to map irrigated areas, land use, land cover, and crop type (Dheeravath et al., 2010; Goetz et al., 2004; Knight et al., 2006; Thenkabail et al., 2005; Varlyguin et al., 2001; Velpuri et al., 2009) and in particular MODIS NDVI time-series data have been used to map both agricultural area (Biggs et al., 2006; Gaur et al., 2008; Gumma et al., 2011a) and seasonal crop area (Sakamoto et al., 2005). These data cover a range of radiometric resolutions (both radar and optical imagery have been used), spatial resolution (sub-national to continental coverage), temporal resolution (single season to multi-year analyses), and thematic resolution (from maps of rice/non-rice to more nuanced assessments of rice agricultural practices).

Synthetic Aperture Radar (SAR) has been used to identify rice areas, and irrigated rice areas in particular. Le Toan et al. (1997) used ERS-1 data for monitoring rice areas and as an input to crop growth simulation models to estimate area and production for study sites of Indonesia and Japan. Similarly, Shao et al. (2001) mapped rice areas using temporal RADARSAT data (1996 and 1997) for production estimates in Zhaoqing in China. Bouvet and Le Toan (2011) demonstrated how lower resolution wide-swath images from advanced SAR (ASAR) data could be used to map rice areas over larger areas. Rice mapping with SAR is advantageous because of pervasive cloud cover across Asia during the months in which much of the rice is cultivated, but the high cost of SAR data in a temporal series has limited its application on a larger scale.

Optical approaches have been commonly used too. Shao et al. (2001) used the Land Surface Water Index (LSWI), enhanced vegetation index (EVI), and normalized vegetation index (NDVI) derived from temporal MODIS data to map rice areas across South and Southeast Asia. Sakamoto et al. (2005) also used EVI derived from MODIS to map rice areas in the Mekong Delta in 2002 and 2003 using wavelet-based filters to determine crop phenology. Nguyen et al. (2012) used SPOT NDVI data with unsupervised classification and field knowledge in the Mekong Delta during 1998–2008. Inoue et al. (2012) used hyperspectral reflectance data by regional assessment of canopy nitrogen content (CNC) at the critical growth stage of the rice crop with various spectral indices, such as the normalized difference spectral index (NDSI) and ratio spectral index (RSI). In almost all the examples listed above, the accuracy assessment of the resulting maps was conducted with limited ground data information for small areas. Furthermore, they generated only rice extent information without any information on differences in rice ecosystems within that extent.

Several studies have used spectral matching technique and/or decision tree algorithms on optical data to obtain information on the different rice cropping systems. Sakamoto et al. (2005) mapped rice areas in South Asia for 2000–01 using MODIS NDVI monthly maximum value composite data with spectral matching techniques (SMTs), but ground data were limited and from a different year than the imagery. Biradar et al. (2009) mapped irrigated and rainfed areas on a global scale at nominal 1 km using AVHRR 10 km, SPOT VGT 1 km, and a suite of secondary data for nominal year 2000. Gumma et al. (2011b) mapped irrigated areas and partitioned between canal and groundwater irrigation areas in the Krishna River basin using MODIS 250 m for 2000–01. However, none of these studies mapped seasonal rice areas. Rice in Asia can be cultivated once, twice, or three times a year, and in more complex cycles such as five crops in two years and seven crops in three years cycles in parts of Vietnam Thailand and Indonesia. We argue that this information gap on cropping intensity and season rice areas can be addressed with existing data and suitable techniques.

1.3. Goal, objectives, and structure

The goal of this paper was to map rice crop extent and areas during three distinct seasons: (*boro* (December/January–April), *aus* (April/May–June/July), and *aman* (July/August–November/December)), for the entire country of Bangladesh based on MODIS 500 m NDVI time-series data using spectral matching techniques, phenological approaches, decision trees, and ground data. The specific objectives were to use MODIS time series data to:

1. Produce seasonal rice extent maps of Bangladesh for 2010.
2. Determine seasonal rice areas at the district level for all 64 districts and for all three seasons in Bangladesh.
3. Establish the accuracies of (a) MODIS-derived rice crop extents by comparing them with independent field data and (b) MODIS-derived rice crop areas by comparing them with independent sub-national statistics.

2. Study area and data

2.1. Study area

Bangladesh is one of the largest rice-growing countries in South Asia. It extends from 20°44′00″ to 26°37′51″N latitude and from 88°0′14″ to 92°40′08″E longitude, and covered 148,450 km^2 (Fig. 1). The country is relatively flat except for the Chittagong Hill Tracts in the Southeast. Most of Bangladesh is covered by the floodplain deltas of three major rivers, the Ganges, Brahmaputra, and Meghna, whose flows discharge into the Bay of Bengal with a combined average of 35,000 $m^3 s^{-1}$ (Islam et al., 2010; WBP, 2012). Floods are a major problem during the monsoon season, and they depend on the duration and magnitude of the rainfall in the upper part of the three major river basins and much of this basin area lies outside Bangladesh. Every year, 25–35% of the total geographic area is inundated by the overflow of rivers during the monsoon season (Islam et al., 2010). Drought and salinity are also major problems especially in the first half of the year. Despite these limitations, the agricultural systems in Bangladesh are complex and take advantage of seasonal environmental variations to cultivate crops throughout the year.

Bangladesh has 8.44 million ha of arable land and 7.81 million ha of net cropped area (BBS, 2006). The total cropped area is 13.75 million ha due to a high cropping intensity of 176%. Rice accounted for 75–76% of the total cropped area between 2003 and 2006; however, it is estimated that rice area had increased to about 84% of the total cropped area by 2008–09 (Asaduzzaman et al., 2010). This suggests that much of the cropping intensity is due to rice, which may be in the form of monoculture or multi-crop systems.

The challenges of increasing productivity are different in each of the three rice seasons that occur in Bangladesh. *Boro* rice (December/January–April) accounts for 50% (5,650,000 ha) of the annual rice production and is the lifeline of Bangladesh. It is cultivated after the previous year's monsoon season, and is dependent on irrigation and high fertilizer inputs to increase production. *Aus* rice (April/May–June/July) accounts for 9% (1,040,000 ha) of the annual rice production and is cultivated on a much smaller area in a period of much higher temperatures. It is cultivated in early monsoon season conditions, in which there is great uncertainly about the onset of the rainy season and hence water availability

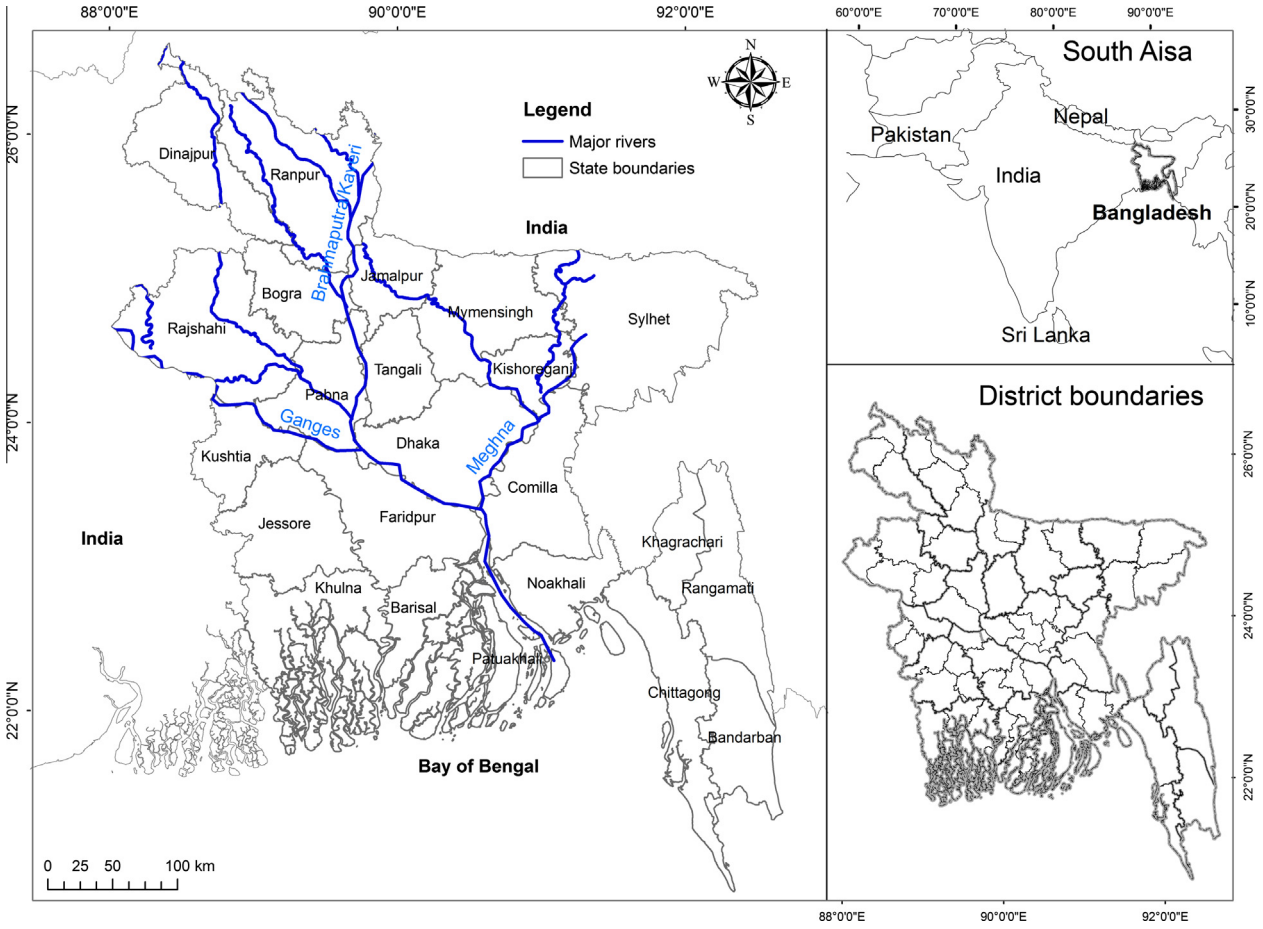

Fig. 1. The Bangladesh study area, showing major rivers and state and district boundaries by location.

is a critical limitation. *Aman* rice (July/August–November/December) accounts for 41% (4,710,000 ha) of the annual rice production and is cultivated in the monsoon season. This crop can suffer from floods or excessive rains (during the early growth period) followed by drought and cool temperatures (during flowering and the reproductive stage).

Climate shocks and unsustainable agricultural practices in Bangladesh have an adverse impact on production and the environment. The land area affected by declining soil fertility, soil erosion, and salinization is estimated at 5.6–8.7 million ha, 5.3 million ha, and 3.05 million ha, respectively (Asaduzzaman et al., 2010). Projected crop areas from climate change models suggest that climate change patterns may increase the negative effect of existing climate variability (Asaduzzaman et al., 2010). This is expected to further reduce rice production, primarily of *boro* rice, by about 3.9% from 2005 to 2050 (Asaduzzaman et al., 2010).

2.2. Data sets

2.2.1. Description of MODIS products used in the study

Moderate-resolution imaging spectroradiometer (MODIS) imagery was downloaded from the Land Processes Distributed Active Archive Center (LP DAAC) (https://lpdaac.usgs.gov/lpdaac/get_data/data_pool). MOD09A1.5 8-day composite, seven-band data for all 46 composite dates (8-day interval) for 2010 were used in this analysis. The spatial resolution of the data is approximately 500 m. Although the data have already undergone atmospheric correction (Vermote and Vermeulen, 1999) and cloud screening, each MODIS 8-day composite was further processed and cloud contamination in each composite was removed (Gumma et al., 2011a; Thenkabail et al., 2005). Cloud contamination can be severe spanning several consecutive 8-day composites, especially during the *aus* and *aman* seasons. We chose to address this by generating monthly composites that would be used alongside the 8-day composites in analysis and interpretation. Interpolation of the 8-day data using gap filling and smoothing algorithms would have been an alternative approach but we had good prior experience with monthly composites and choose that approach instead of selecting from a range of smoothing algorithms.

MODIS 8-day composites were used to calculate three indices: (a) NDVI, (b) NDVI monthly maximum value composites (NDVI MVC) and (c) Land Surface Water Index (LSWI), using surface reflectance values from the red (620–670 nm) NIR1 (841–875 nm) and SWIR1 (1628–1652 nm) bands with the following equations:

$$NDVI = \frac{(\lambda_{NIR} - \lambda_{red})}{(\lambda_{NIR} + \lambda_{red})} \quad (1)$$

$$NDVI_{MVCI} = Max(NDVIi_1, NDVIi_2, NDVIi_3, NDVIi_4) \quad (2)$$

$$LSWI = \frac{(\lambda_{NIR} - \lambda_{swir})}{(\lambda_{NIR} + \lambda_{swir})} \quad (3)$$

where MVC_i is the monthly maximum value composite of the ith month and i_1, i_2, i_3, and i_4 are every 8 days' data in a month. Monthly NDVI MVC were used for classification, NDVI 8-day data were used for identifying and labeling seasonal rice classes and LSWI data were used to help resolve mixed classes.

2.2.2. Sampled field-plot information for groundtruth

Sampled field-plot information was gathered from 605 locations during August 4–18, 2010. Local agricultural officers accompanied the lead author during the field visit and farmers were interviewed and/or local experts provided inputs at each location. The representativeness of the field samples is based on local expert knowledge and our field observations. Some areas of the country could not be visited due to time constraints and lack of access due to monsoon rains.

The following data were collected at 191 out of the 605 locations: (a) geographic location using a handheld GPS unit, (b) crop type, (c) cropping season (*boro-rice*, *aus-rice*, and *aman-rice*) based on interviews with agricultural extension officers and farmers, (d) cropping patterns, (e) land holding size, small ($\leqslant$10 ha), medium (10–15 ha), and large ($\geqslant$15 ha), (f) land cover categories, (g) source of water by season and (h) digital photographs (Fig. 2). For the remaining 414 points we recorded only the geographic coordinates, cropping pattern/intensity, and digital photographs.

The 191 points that had detailed field data were used for class identification and calculating rice fractions (a visual estimate of the percentage area covered by rice from centre of a 500 m pixel for a field observation point). Of those 191 points, 156 were dominated by rice and 35 points had other land cover. Within the 156 rice points, 118 were used to generate 15 ideal temporal profiles of distinct rice ecosystems while the remaining 38 were mixed rice classes. Furthermore, within those same 156 rice points, we identified rice in 103 locations in the *boro* season, 12 locations in the *aus* season, and 117 locations in the *aman* season, demonstrating that our fieldwork captured areas where rice cropping intensity was greater than 100%. The *aus* season is slightly under represented in the field observation data considering the reported rice area per season. This reflects the fragmented *aus* distribution and highlights the challenge of capturing such spatial patterns in a rapid field campaign.

The 414 points with limited observations used for the classification accuracy assessment (validations points). Again, we sufficiently captured areas of high cropping intensity: 269 observations of *boro*, 99 of *aus*, and 303 of *aman* rice (the remaining points were other land use/land cover).

Field-plot locations were selected based on the homogeneity of locations and road access. The emphasis was on "representativeness" of the sample location in representing one of the classes to ensure precise geo-location of the pixel. Class labels were assigned in the field using a labeling protocol (see Thenkabail et al., 2009).

2.2.3. Sub-national rice area statistics – secondary data

Rice area statistics for 2010 were obtained from the Bangladesh Bureau of Statistics (BBS, 2011) for 64 districts, the most detailed sub-national administrative unit for which seasonal rice area estimates were available for 2010. The BBS reports also contained useful contextual information on changes in area and production from past years and offered general comments on the reasons for those changes, such as higher rainfall, adoption of improved varieties, or rehabilitation of the irrigation system.

3. Methods

The seasonal rice mapping methodology (Fig. 3) involved the following ten steps:

(3.1) Temporal series of reflectance data.
(3.2) Generating class spectra by performing an unsupervised classification on NDVI MVC.
(3.3) Composing an ideal spectral data bank.
(3.4) Grouping classes with a decision tree algorithm.
(3.5) Grouping classes with spectral similarity values.
(3.6) Spectral matching techniques.
(3.7) Identifying and labeling classes.
(3.8) Resolving mixed classes.
(3.9) Sub pixel area estimation.
(3.10) Accuracy assessment.

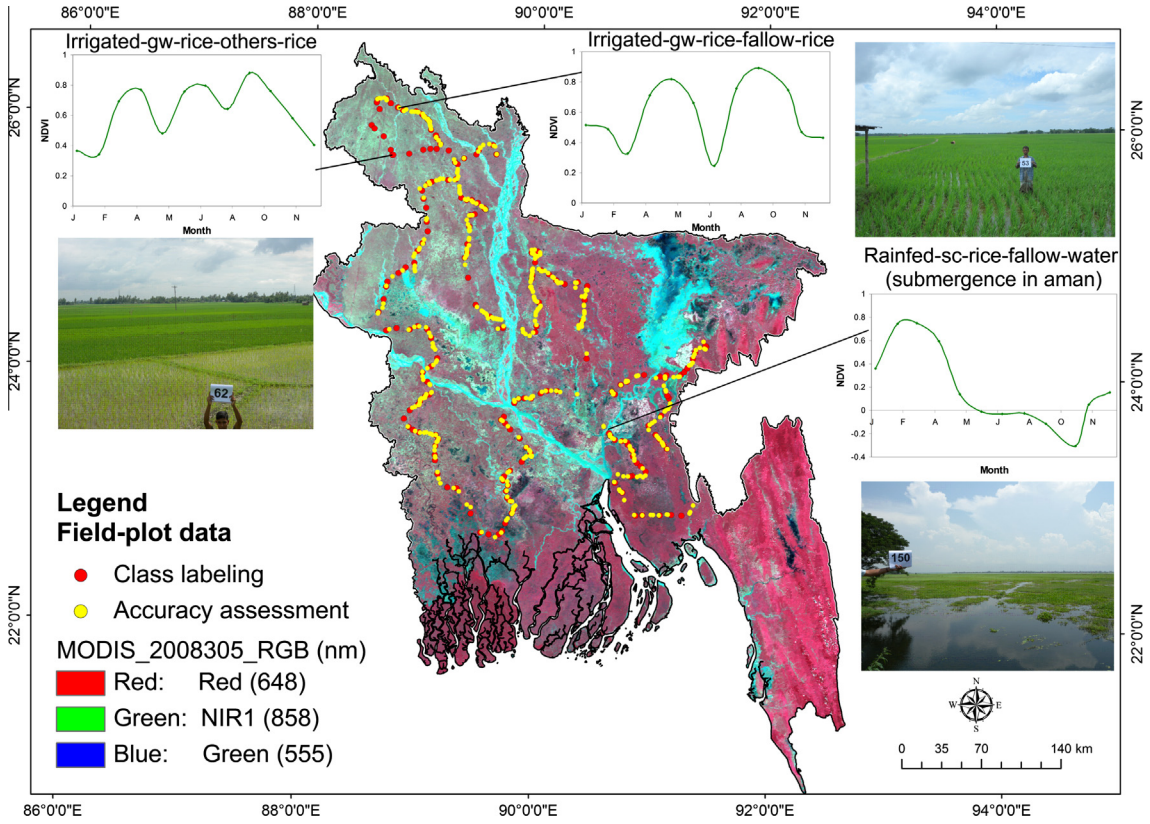

Fig. 2. Field-plot data-point locations in Bangladesh. There are 605 field-plot locations where data on crop type, cropping intensity, water source (irrigated versus rainfed), and a number of other parameters (e.g., crop planting dates and harvest dates) were collected with sample NDVI signatures of rice-growing areas (irrigated-GW-rice-rice-rice-LS, irrigated-GW-rice-fallow-rice-LS, and deepwater-rice-water-fallow-LS).

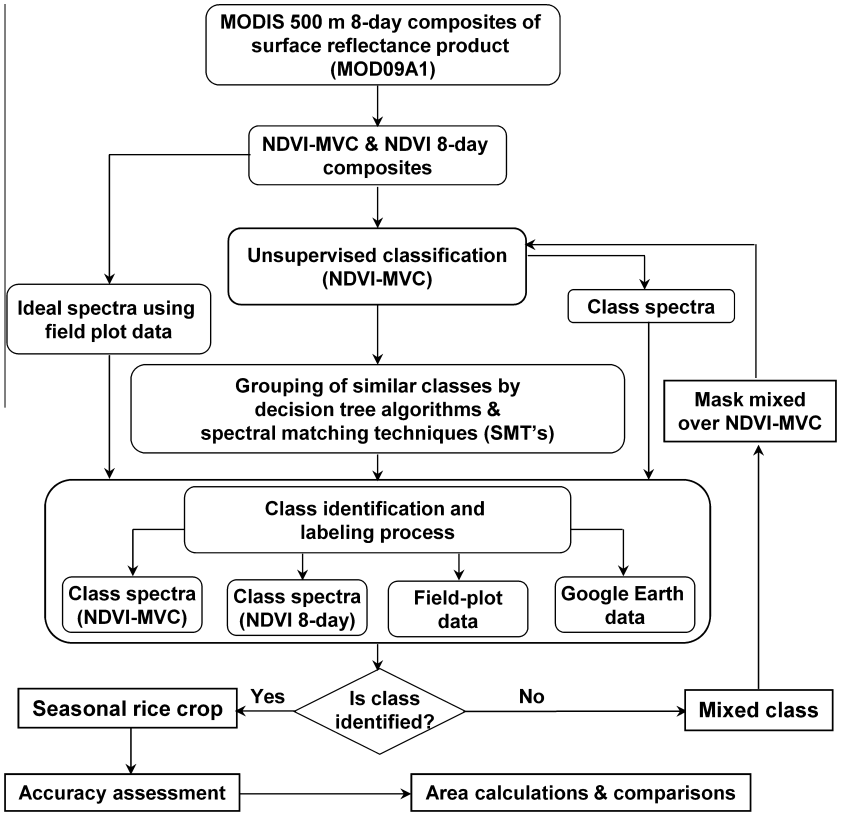

Fig. 3. Overview of the methodology for mapping rice areas using the 8-day MODIS 500 m MOD09A1 data and other ancillary spatial data.

3.1. Temporal reflectance data and NDVI data

A 315 layer stack of reflectance data for all seven bands for across 46 weeks was generated using MODIS imagery (Thenkabail et al., 2009). The 8-day NDVI images were prepared by using Eq. (1)and monthly MVCs of NDVI for January through December (12 layer stack) was prepared using Eq. (2).

3.2. Generating class spectra by performing an unsupervised classification on NDVI MVC

Class spectra (e.g., Fig. 4b1) were generated through an unsupervised ISODATA cluster algorithm on the 12-band monthly MVC NDVI. Unsupervised classification was used instead of supervised classification in order to capture the range of variability in phenology over the study area, particularly in large study areas where the NDVI signatures of most of the potential classes are unknown. The unsupervised classification was set at a maximum of 100 iterations with a convergence threshold of 0.99 (Leica, 2010). ISODATA classification using progressive generalization led to an initial 100 classes (Cihlar et al., 1998). The MODIS NDVI time-series spectra were then plotted for each of the 100 classes for labeling.

3.3. Composing an ideal spectral data bank

Ideal spectral signatures were generated using time-series data that were extracted from 118 observation points (see Fig. 2 and Section 2.2.2). Each of the points chosen to generate the ideal spectral signatures (e.g., Fig. 4b2) represents a definitive crop type and/or cropping system such as "irrigated-groundwater-rice-rice-rice" (meaning the rice field is irrigated by groundwater and is rice during all three seasons), "irrigated-groundwater-rice-fallow-rice", or "deepwater-rice-fallow-water". Multiple points with the same crop type/system, even though distributed spatially in discrete patches were combined to create a single ideal spectral signature (e.g., Fig. 4b2), for that cropping system (between 5 and 17 points per spectra) resulting in 15 ideal rice signatures and a 9 ideal signatures for other classes.

3.4. Grouping classes with a decision tree algorithm

A decision tree was applied to the 100 NDVI signatures (Fig. 4a) obtained from 100 classes that resulted from the unsupervised classification to obtain twelve distinct groups. The decision tree is based on monthly NDVI thresholds at different crop growth stages in the season. The months and threshold values were chosen based on knowledge of the crop calendar from local experts, field observations as well as published rice crop development stages (Fig. 4a).

3.5. Subsequent grouping of classes using spectral similarity values

There are several spectral matching techniques (SMTs) (Thenkabail et al., 2007) to reduce the grouping into similar land use classes, and in this case we selected spectral similarity value (SSV) (Homayouni and Roux, 2003) that has previously performed well in analyzing spectral signatures for agricultural crops such as rice (Thenkabail et al., 2007). SSV was calculated for each class combination,

$$SSV = \sqrt{ED^2 + (1 - \rho)} \quad (4)$$

where ED is the Euclidian distance and ρ is the correlation coefficient between the ideal and class temporal signatures. The lower the SSV value the higher the similarity between the two classes.

3.6. Spectral matching technique

Classes with similar SSVs were grouped and then matched against ideal spectra (Fig. 4b). The 100 classes obtained from the unsupervised classification include crop and non-crop lands. Each of those classes was investigated and grouped into similar or near-similar broad classes. We use an example to illustrate the process base on nine similar cropland classes obtained by the DT algorithm in Fig. 4b1, Section 3.4. The nine classes (class numbers 24, 40, 41, 45, 47, 50, 52, 54, and 59) have similar or near-similar signatures as determined by their SSVs. The nine classes are then matched with the nearest ideal signature (Fig. 4b2). This resulted in three class spectra (classes 41, 45, 47) matching perfectly with ideal spectra "4", which is labeled as "irrigated-surface water – double crop – rice in *boro* season – fallow in *aus* season – rice in *aman* season – large scale" (Fig. 4b3). The same process is followed for all cropland classes until all class spectra are matched to ideal spectra.

3.7. Identifying and labeling classes

The combination of decision trees and spectral matching allows for rapid and accurate identification and labeling of classes as illustrated in Fig. 4a. However, further affirmation of the class labeling requires steps B through D especially in cases where we did not have a sufficiently rich ideal spectral data bank. Whenever there was ambiguity in the class matching we used various sources of information to increase our confidence in the matching decision. We performed visual interpretation of the phenology from the 8-day NDVI and LSWI time-series to distinguish between irrigated and rainfed systems or to confirm deepwater systems for example. We also relied on visual interpretation of high resolution imagery from Google Earth (where available) to confirm the presence of any rice bunds or irrigation structures. Finally we referred back to relevant information from our field plot data to correctly class match the class. These steps are illustrated in Fig. 4c.

3.8. Resolving mixed classes

When a study area contains many distinct land cover classes over a large spatial extent, there is a risk that some of the classes from the unsupervised classification may contain several sub-classes or mixed classes. These mixed classes were resolved by extracting them from the stack, reclassifying them, and applying the methodology above on these new classes in order to separate them.

3.9. Sub-pixel area estimation

With the use of moderate spatial resolution imagery in areas where land use patterns change over sub-pixel distances, it is inevitable that many MODIS pixels will contain more than one land cover class. The labeling of classified land cover maps at this resolution suggests that each pixel in that class is 100% pure, when this is certainly not always the case. One approach is to use higher resolution imagery with spectral and spatial resolutions capable of accurate rice area estimation. This requires a sample of imagery across the study site that captures representative rice classes in each season. Since this was beyond the scope of this study we estimated the sub-pixel rice area for each rice class from the 191 detailed ground data observations following previous methods (Thenkabail et al., 2007).

The ground data observations include a visual estimate of the proportion of the 500 m × 500 m area that surrounds the observation point under different land use (water, built-up area, cropland, etc.). If our ground data observations are representative of the rice

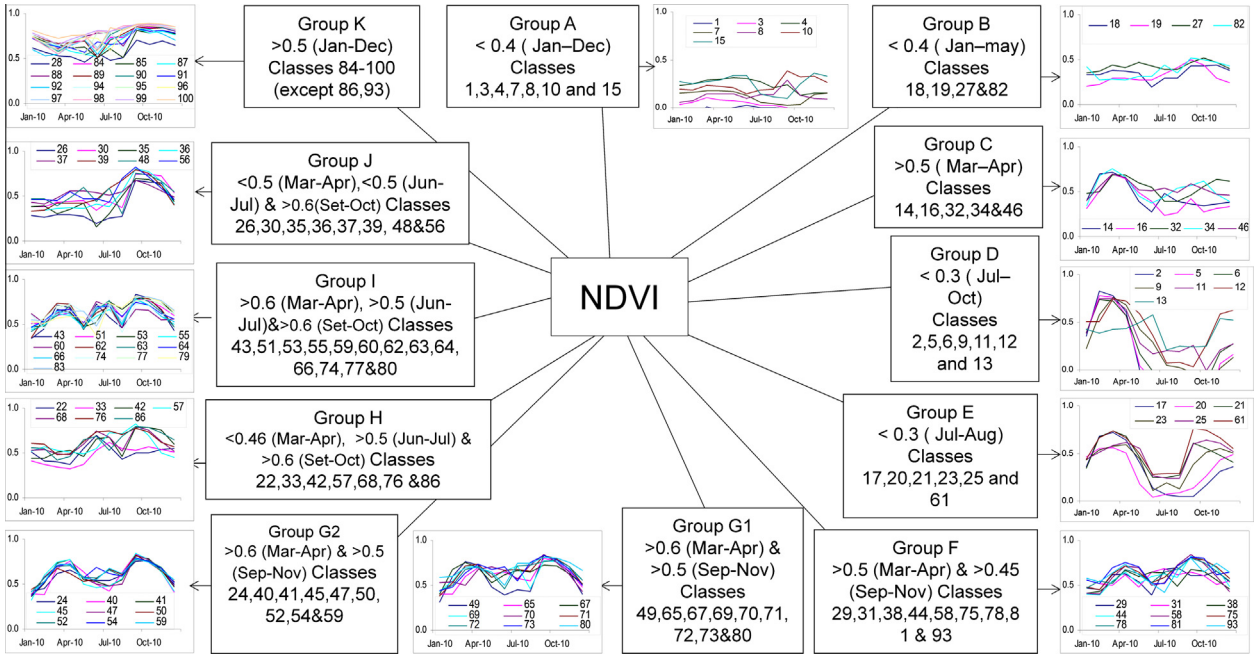

Fig. 4a. Decision tree algorithm to group and identify classes. MODIS monthly NDVI MVC classes are plotted and grouped.

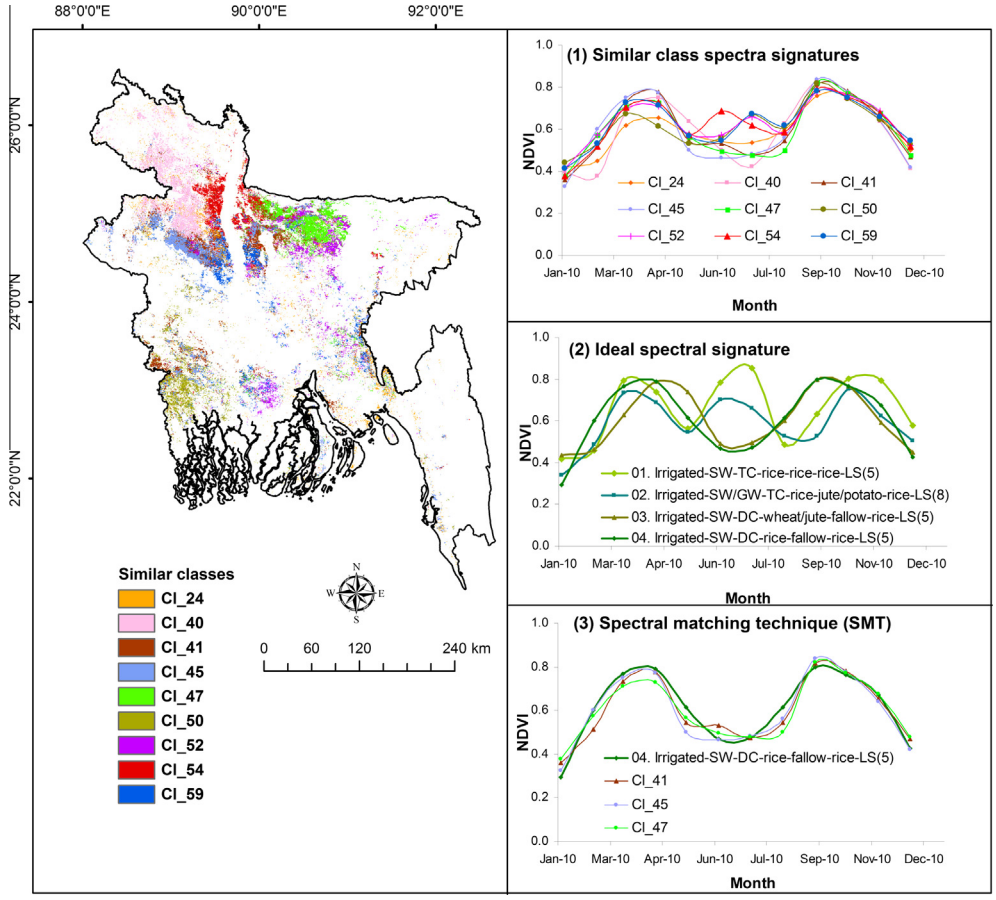

Fig. 4b. Spectral matching techniques (SMTs) illustrated. The MODIS NDVI MVC images were classified to obtain class spectra. Of the 100 initial classes, we illustrate here MODIS monthly NDVI MVC class spectra for nine classes (e.g., Fig. 4a1). The four ideal spectral signatures (Fig. 4a2) are illustrated from the ideal spectral data bank generated based on exact knowledge from field-plot data (Fig. 2) and MODIS monthly NDVI signatures from these locations. The class spectra (e.g., Fig. 4a1) are then matched (e.g., Fig. 4a3) with ideal spectra (e.g., Fig. 4a2) to identify and label classes. Fig. 4a3 shows a simple qualitative match between ideal spectra number 4 with class spectra classes 41, 45, and 47. So, class spectra classes 41, 45, and 47 take the same name as ideal spectra number 4 ("Irrigated-SW-DC-rice-fallow-rice-LS").

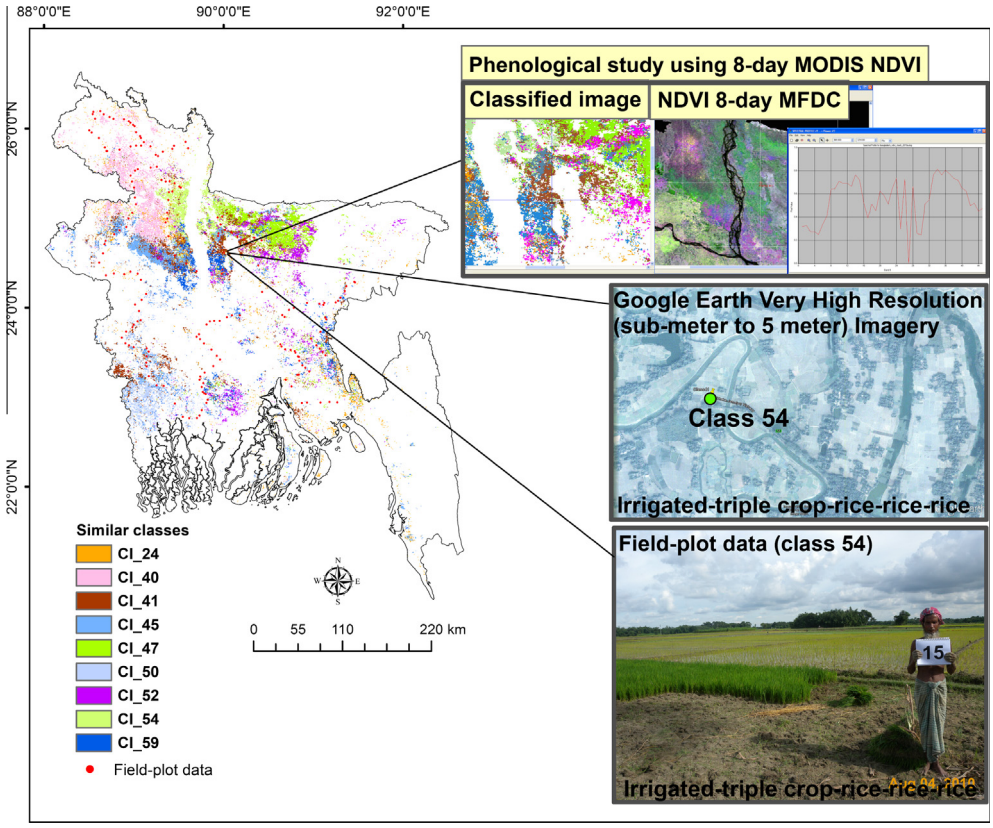

Fig. 4c. Use of MODIS 8-day phenology and very high resolution (sub-meter to 5-m) imagery in class identification and labeling.

systems and we have sufficient observation points per class, then we can estimate a reliable rice area fraction (sub pixel area, or SPA) for each class based on the average rice area across all observation points in that class. The SPA information is applied to each class to estimate the actual rice area for that class. This SPA rice area estimate is compared with the published sub-national rice area rather than the MODIS pixel rice area. As seen in Section 3.2, the number of field points per rice season is not proportional to the published rice area statistics. If we assume that the statistics are an accurate assessment at district level – an important assumption for our area accuracy assessment – then care must be taken when interpreting the SPA for those under represented classes.

3.10. Rice classification accuracy assessment

The 414 field-plot points were used to assess the accuracy of the classification results, based on a theoretical description given by Jensen (2004), to generate an error matrix and accuracy measures for each seasonal rice map.

4. Results

4.1. MODIS derived seasonal rice maps and area statistics

For each season – *boro*, *aus* and *aman* – we identified, labeled (Fig. 5) and estimated the area of up to five rice classes (Table 1). Class one is rainfed, classes two to four are irrigated, while class five is rice with a long period of flooding prior to rice emergence that could be termed deepwater rice. Of the three irrigated classes, class two is groundwater irrigated, class three is a combination of groundwater and surface-water irrigation and class four is surface-water irrigated. The final class name or label (Fig. 5 and Table 1) is based on the predominance of a particular land cover (e.g., trees, grasses, shrubs, other crops) within the rice class. The rice area, including season-wise area and percentage of total geographic area, is shown in Table 1.

The total net rice area (SPA), for the year 2010 based on MODIS data, from the three seasons combined is 8,004,961 ha (Fig. 5 and Table 1) whereas the annualized rice area (from all three seasons combined) is 11,931,708 ha, resulting in a rice cropping intensity of 1.49. Although from a different year our area estimate is 15% lower and our cropping intensity is 0.27 lower than those by Asaduzzaman et al. (2010).

4.2. Temporal MODIS signatures for seasonal rice classes

Boro, *aus*, and *aman* rice-growing areas have shown very good separation in the classification (Fig. 6a–c). In Fig. 6a, the class "01. Rainfed-rice" signature extends from January to May, with high NDVI values between February and March, indicating *boro* rice, followed by *aus* rice. In Fig. 6b, the class signatures extend from May to July, with high NDVI values between June and July, indicating *aus* rice, and, later in the season, very low NDVI. In Fig. 6c, the class "05. Deepwater-rice" signature extends from mid-June to August, with significantly low NDVI values, which indicates submergence during the start of the *aman* season, followed by rice crop growth from September to December.

4.3. Accuracies, errors, and uncertainties

Table 2 shows the error matrices for each season. In the *boro* season, for class one, only three of the five points matched perfectly and the other two points matched with irrigated-groundwater-rice, where as for class two, 213 out of 238 points matched with the same class with the main error was related to

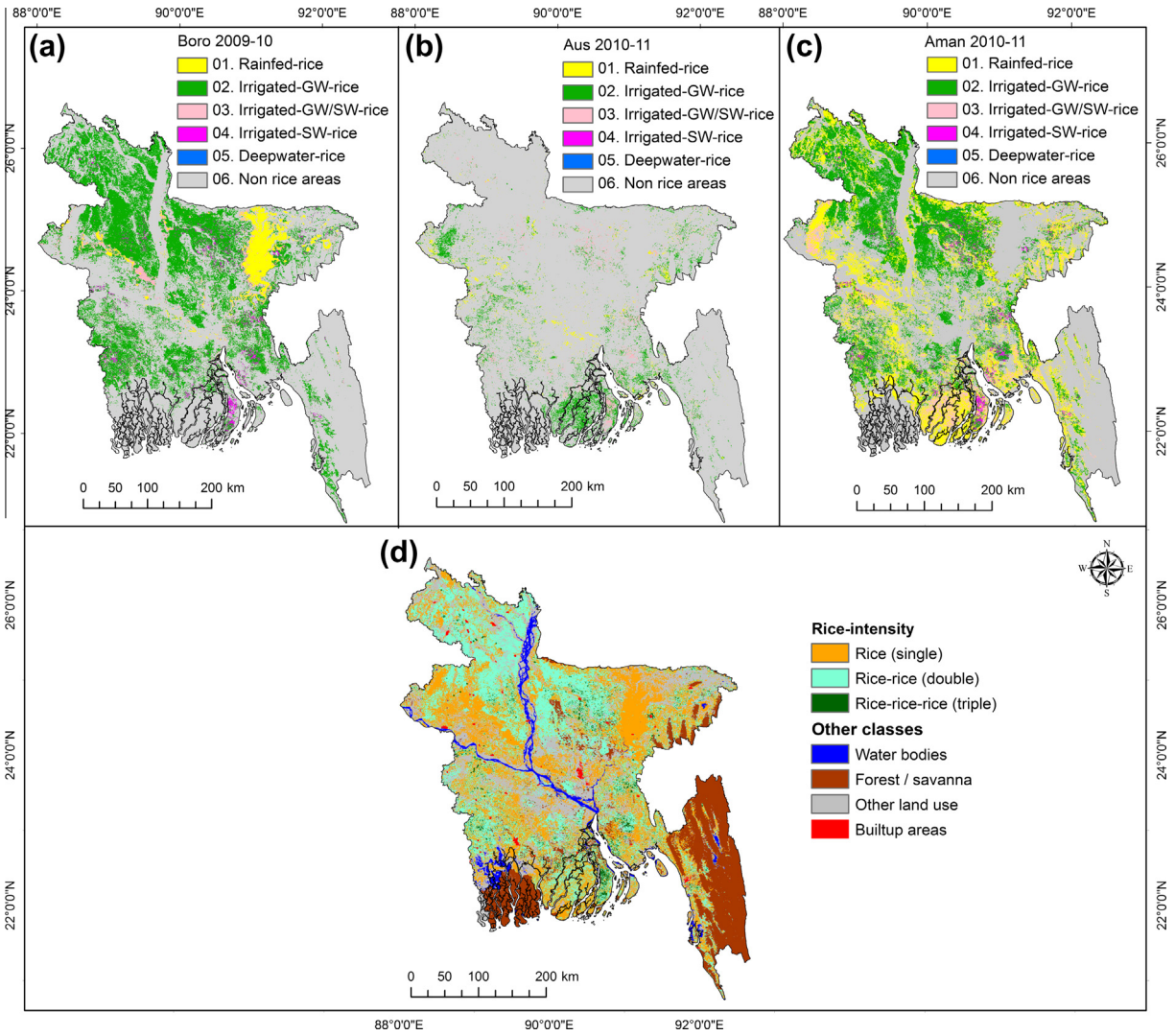

Fig. 5. Spatial distribution of rice cultivation with season and irrigation source. (a) Spatial distribution of *boro*, (b) *aus*, (c) *aman* rice, and (d) net rice with other land use/land cover.

misclassified non-rice areas. The same assessment can be made for each class and season. The overall accuracy for the *boro* season was 82.13% with a Kappa value of 0.66. For *aus* the same figures were 90% and 0.70 whilst for *aman* they were 78% and 0.64.

4.4. Comparison with sub-national statistics and other published rice area estimates

The final classified maps of seasonal rice areas were compared against district-level rice area (Table 3). On average, the MODIS-derived rice area had slightly higher estimates: higher by 7% during *boro*, 6% in *aus* and by 3% during *aman*. This overestimation is clear in the scatterplots of district level area estimates (Fig. 7) and the root mean squared error between the two area estimates (9556 ha for *boro*, 3754 ha for *aus*, and 11,349 ha for *aman*).

5. Discussion and conclusions

5.1. Discussion on results: seasonal rice maps and area estimates

Rice is grown extensively during the *aman* season, resulting in a total rice area for the season of 5,816,240 ha from MODIS or 5,645,640 ha from the published national statistics, which is nearly 40% of the total geographic area of the country. Not only are the rains abundant during the monsoon, but also flooding from the Ganges and Brahmaputra is extensive. This results in groundwater recharge and saturation of soils, making water available for rice in abundance.

A unique feature during the *aman* season is deepwater rice (35,565 ha during 2010; Fig. 5 and Table 1). These rice fields remain completely under water for anywhere from 1 to 2 months because of heavy flooding from the two great rivers.

The *aman* season is followed by the dry *boro* season (5,011,631 ha, from MODIS or 4,706,874 ha from published national statistics), when rains are infrequent but soil moisture is still high and there is abundant or adequate shallow ground water throughout large parts of the country. This results in a high percentage of groundwater irrigated rice area during this season (4,143,590 ha out of 5,011,631 ha from MODIS). *Boro* rice areas are spatially located in the Bogra, Comilla, Jamalpur, Mymensingh, and Ranpur regions.

Aus (dry season) cultivation of rice is smaller than *boro* or *aman* (1,103,738 ha from MODIS and 1,035,578 ha from published national statistics) and occurs only in areas where there is sufficient water from irrigation to establish a crop. Although the latter part of

Table 1
Rice classes during the three seasons in a year. The actual rice area shown in the last column is obtained by multiplying the full-pixel areas of each class by the rice area fraction of that class.

Rice classes	Full-pixel area (ha)	Rice fraction (%)	Sample size	Land cover areas within the classes (ha)					
				Trees	Grasses	Water	Shrubs	Other crops	Actual rice area (= sub-pixel area)
Boro(December/January–April)									
01. Rainfed-rice	502,291	100	10	–	–	–	1507	–	500,723
02. Irrigated-GW-rice	4,428,126	94	75	146,060	53,138	26,312	29,859	27,485	4,143,590
03. Irrigated-GW/SW-rice	137,642	99	7	688	138	–	275	413	136,185
04. Irrigated-SW-rice	241,977	96	11	2819	3213	4027	726	–	231,133
05. Deepwater-rice	0	0	0	0	0	0	0	0	0
Aus (April/May–June/July)									
01. Rainfed-rice	168,837	97	4	1266	422	844	0	1688	164,616
02. Irrigated-GW-rice	781,847	90	5	688	138	40,268	32,352	413	707,989
03. Irrigated-GW/SW-rice	241,594	96	3	2819	3213	4027	403	0	231,133
04. Irrigated-SW-rice	0	0	0	0	0	0	0	0	0
05. Deepwater-rice	0	0	0	0	0	0	0	0	0
Aman (July/August–November/December)									
01. Rainfed-rice	2,431,102	83	4	99,675	55,915	100,822	29,173	19,449	2,126,068
02. Irrigated-GW-rice	3,171,026	84	56	31,711	34,881	157,102	44,394	34,564	2,868,373
03. Irrigated-GW/SW-rice	646,563	79	41	19,461	16,228	32,351	4849	14,225	559,449
04. Irrigated-SW-rice	243,140	85	11	3404	2188	7286	1775	1702	226,785
05. Deepwater-rice	46,090	89	5	4102	1106	4027	876	415	35,565
Boro rice									5,011,631
Aus rice									1,103,738
Aman rice									5,816,240
Total rice area (*boro* + *aus* + *aman*) or annualized rice area (see Fig. 5)									11,931,608
Net rice area (see Fig. 5d)									8,004,961

the season can also be irrigated in the limited areas that have sufficient water, the majority of *aus* rice relies on early monsoon rains for the remainder of the season, making this a drought prone crop. This reliance on post *boro* season irrigation and higher risk of drought are two reasons why *aus* has a limited extent and a spatially fragmented pattern across Patuakhali, Rajshahi, and Noakhali regions.

Bangladesh has a predominance of groundwater irrigation as is evident from the large area of class two (Fig. 5 and Table 1) in all three seasons; 4,143,590 ha in *boro*, 707,989 ha in *aus*, and 2,868,373 ha in *aman* and this deserves further discussion. The *aus* crop often relies on irrigation to establish the crop and then on early monsoon rains for the remainder of the season. *Aman* is essentially a rainfed crop, but when there is a shortfall in rain then groundwater may be used as supplemental irrigation. However, irrigation use in *aman* is very small compared to *boro* and *aus* and the presence of a large area of class two in the *aman* season map should not be interpreted as areas of *aman* rice that rely entirely on irrigation. What is clear is that many parts of Bangladesh become flooded during the monsoon, resulting in recharge of groundwater. This has resulted in many shallow groundwater wells from which water is used to irrigate rice fields. The heavy use of this recharge water takes place in the months immediately after the monsoon during the *boro* season (from December/January to April) and is the reason why class two area is highest during *boro*.

The district-wise rice area derived from our study was compared with national statistics (BBS, 2011) and there was a very good correlation between the two (*boro*: $R^2 = 0.962$, *aus*: $R^2 = 0.934$, *aman* $R^2 = 0.963$, and no. of districts = 64). The main advantage of the remote sensing based area estimates is the availability of area data at finer granularity than the published statistics such that we can interpret them at a pseudo field level to generate cropping intensity information within each district.

The three rice seasons per year can be combined in seven possible rice cropping patterns across those seasons (*boro*, *aus*, *aman*, *boro-aus*, *boro-aman*, *aus-aman*, and *boro-aus-aman*). Such seasonal mapping will have huge implication in determining water use by crops with greater accuracies. Given Asia's importance in agricultural output, and the high cropping intensity, mapping croplands by season is a key component in modeling resource use and land use intensity, especially water. Rice crop productivity and water productivity vary by season and capturing these dynamics and capturing the intra annual spatial and temporal patterns of crop extent aids our understanding of seasonal cropland and water use dynamics.

Our study has successfully mapped rice areas and season-wise rice areas and adequately classified rainfed and irrigated environments mainly in the northern, western, and central regions of the study area, where a clear difference between rainfed and irrigated rice temporal signatures was detected. However, there were some areas where correct classification was challenging. Rice areas with high rainfall were mixed with irrigated rice areas, particularly in the *aman* season. Separating the spectral signatures from irrigated rice areas and favorable rainfed rice areas is difficult without auxiliary information on irrigation infrastructure. Also the landscape in three coastal divisions Khulna, Barisal and Patuakhali is challenging to map accurately with MODIS and exacerbated by the lack of field data in many of the coastal districts. It is a poor region with small landholdings and much of the agriculture takes place within polders that aim to control water flow. There are large areas of aquaculture and shrimp cultivation in the highly saline dry season, and homesteads, villages and dense, tree lined canal and river networks contribute to a highly mixed pixel environment at MODIS resolution. Any MODIS based classification of this area is challenging.

5.2. Discussion on methods

Classification of remote sensing imagery requires several decisions on the most appropriate methods and thresholds used in those methods. In the case of supervised methods, they also rely on subjective operator interventions to derive the best result. Here

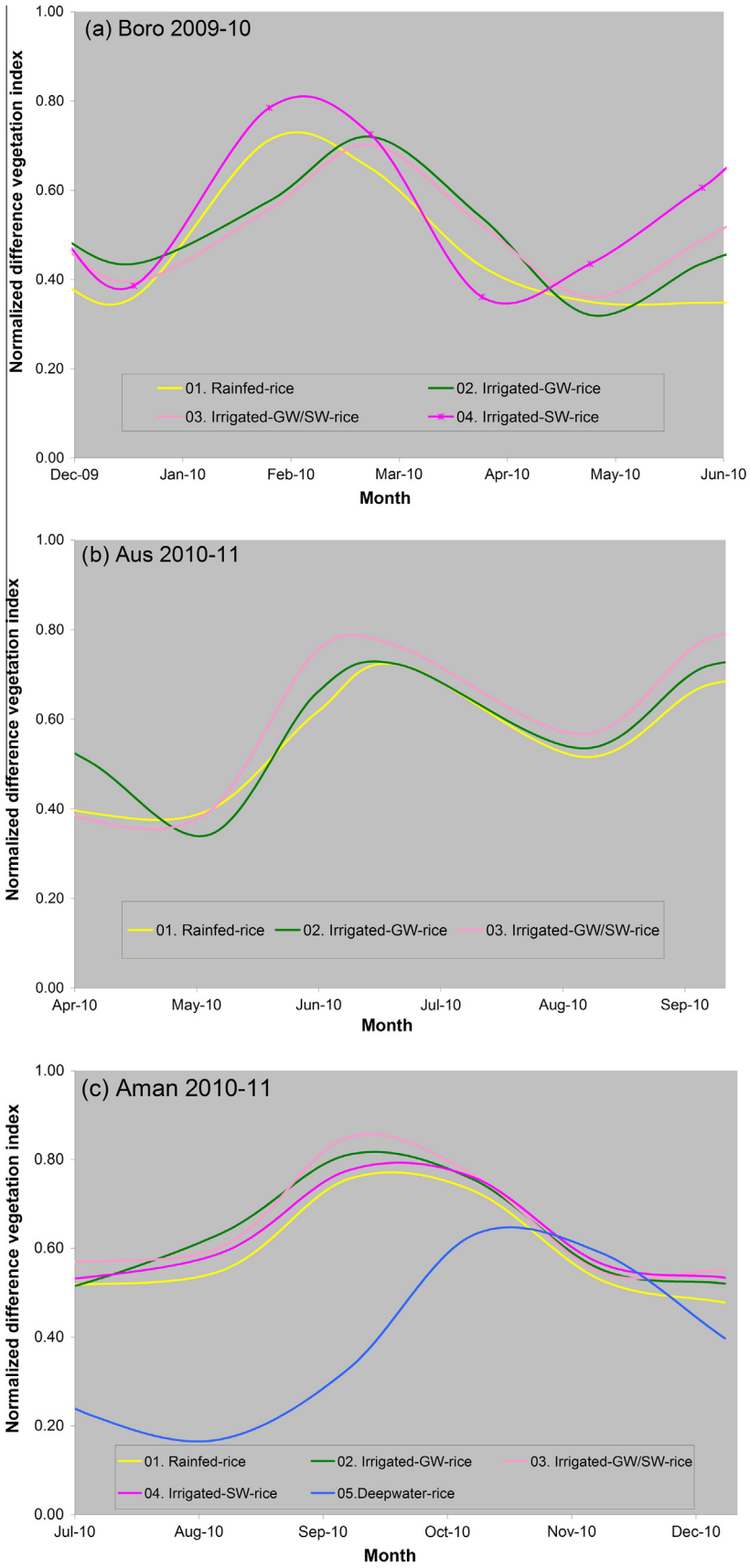

Fig. 6. Temporal mean MODIS 500 m NDVI signatures of the five rice classes for the three seasons for 2010. These NDVI signatures are for the classes in Fig. 5. *Note*: when a particular class does not exist in a season, then naturally that class will not have an NDVI signature.

Table 2
Accuracy assessment using field-plot data.

Rice classes	Reference data (field-plot data)							Reference totals	Classified totals	Number correct	Producers' accuracy	Users' accuracy	Kappa
	01. Rainfed-rice	02. Irrigated-GW-rice	03. Irrigated-GW/SW-rice	04. Irrigated-SW-rice	05. Deepwater-rice	06. Nonrice area	Row total						
Boro													
01. Rainfed-rice	**3**	0	0	0	0	0	3	5	3	3	60%	100%	1.0
02. Irrigated-GW-rice	2	**213**	8	2	3	25	253	238	253	213	90%	84%	0.6
03. Irrigated-GW/SW-rice	0	2	**3**	3	0	1	9	13	9	3	23%	33%	0.3
04. Irrigated-SW-rice	0	1	0	**2**	0	0	3	10	3	2	20%	67%	0.7
05. Deepwater-rice	0	0	0	0	**0**	0	0	3	0	0	–	–	0.0
06. Non-rice area	0	22	2	3	0	**119**	146	145	146	119	82%	82%	0.7
Column total	**5**	**238**	**13**	**10**	**3**	**145**	**414**	**414**	**414**	**340**			
Overall classification accuracy = 82%								Overall Kappa statistics = 0.6590					
Aus													
01. Rainfed-rice	**2**	0	0	0	0	0	2	10	2	2	20%	100%	1.0
02. Irrigated-GW-rice	0	**13**	2	0	0	2	17	28	17	13	46%	76%	0.7
03. Irrigated-GW/SW-rice	2	1	**44**	0	0	1	48	54	48	44	81%	92%	0.9
04. Irrigated-SW-rice	0	0	0	**0**	0	0	0	7	0	0	–	–	0.0
05. Deepwater-rice	0	0	0	0	**0**	0	0	0	0	0	–	–	0.0
06. Non-rice area	6	14	8	7	0	**312**	347	315	347	312	99%	90%	0.6
Column total	**10**	**28**	**54**	**7**	**0**	**315**	**414**	**414**	**414**	**371**			
Overall classification accuracy = 90%								Overall Kappa statistics = 0.7017					
Aman													
01. Rainfed-rice	**56**	10	1	0	0	9	76	86	76	56	65%	74%	0.7
02. Irrigated-GW-rice	20	**172**	2	6	1	13	214	199	214	172	86%	80%	0.6
03. Irrigated-GW/SW-rice	0	0	**0**	0	0	0	0	3	0	0	–	–	0.0
04. Irrigated-SW-rice	0	1	0	**2**	0	0	3	11	3	2	18%	67%	0.7
05. Deepwater-rice	0	0	0	0	**3**	0	3	4	3	3	75%	100%	1.0
06. Non-rice area	10	16	0	3	0	**89**	118	111	118	89	80%	75%	0.7
Column total	**86**	**199**	**3**	**11**	**4**	**111**	**414**	**414**	**414**	**322**			
Overall classification accuracy = 78%								Overall Kappa statistics = 0.6383					

Figures in bold are column totals and the diagonals in the confusion matrices.

Table 3
Comparison of MODIS rice area estimates with sub-national statistics by district and season.

Region	National statistics				MODIS rice areas			
	Boro[a]	*Aus*[b]	*Aman*[c]	Total	*Boro*	*Aus*	*Aman*	Total
Bandarban	3161	6230	8191	17,582	1577	8284	12,612	22,474
Barisal	91,013	84,572	242,685	418,270	121,383	69,930	250,789	442,103
Bogra	258,367	18,078	251,603	528,048	283,833	28,260	252,674	564,767
Chittagong	119,405	43,630	260,251	423,286	127,491	43,156	271,491	442,138
Comilla	341,171	81,119	262,429	684,719	347,357	74,824	260,985	683,165
Dhaka	280,739	4784	170,707	456,230	298,290	11,688	177,808	487,787
Dinajpur	286,916	4415	445,946	737,277	313,737	15,846	440,779	770,362
Faridpur	212,326	31,546	182,595	426,467	214,161	52,205	182,605	448,970
Jamalpur	217,265	8636	193,574	419,475	201,596	10,025	237,353	448,974
Jessore	326,230	85,954	314,443	726,627	345,243	78,035	346,177	769,454
Khagrachari	10,064	2457	30,611	43,132	10,225	3084	30,534	43,843
Khulna	161,202	23,637	273,432	458,271	151,090	23,330	266,163	440,584
Kishoreganj	312,969	23,041	214,623	550,633	187,652	16,802	83,323	287,777
Kushtia	99,382	54,730	146,770	300,882	109,970	61,414	178,985	350,369
Mymensingh	257,926	51,051	273,270	582,247	441,591	63,943	425,341	930,875
Noakhali	118,820	86,560	269,434	474,814	129,746	92,929	258,696	481,371
Pabna	202,830	26,597	174,687	404,114	196,410	28,144	192,773	417,326
Patuakhali	59,672	179,194	476,977	715,843	61,714	169,916	427,236	658,867
Rajshahi	372,370	122,892	384,316	879,578	369,386	126,544	406,323	902,252
Rangamati	7359	5768	9541	22,668	7720	4799	18,210	30,729
Ranpur	464,189	355	546,979	1,011,523	475,030	2611	571,896	1,049,537
Sylhet	339,074	89,347	370,009	798,430	445,919	115,521	373,499	934,939
Tangali	164,424	985	142,567	307,976	170,508	2449	149989	322,946
Total rice area	4,706,874	1,035,578	5,645,640	11,388,092	5,011,631	1,103,738	5,816,240	11,931,608
RMSE					9596	46,079	98,982	258,747
NRMSE					2%	26%	18%	26%

Note: we tabulate the areas using the older and larger 23 districts of Bangladesh for reasons of space. The scatterplots in Fig. 7 show the results for the 64 districts.
Source:
[a] www.bbs.gov.bd/webtestapplication/userfiles/image/AgricultureCensus/*Boro*-2010-11.pdf.
[b] www.bbs.gov.bd/webtestapplication/userfiles/images/AgricultureCensus/*Aus*10_11pdf.
[c] www.bbs.gov.bd/webtestapplication/userfiles/image/AgricultureCensus/*Aman*-%202010-11.pdf.

we discuss the different choices that were made in the development of the methodology, the advantages and disadvantages, and, some indications of how the approach can be improved.

The decision to use hyper temporal MODIS imagery is based on the need to capture three distinct seasons of a crop which is known to cover a large proportion of the study area in a region with pervasive cloud cover. The 8-day and monthly composites provide a good basis for capturing the seasonal variability in vegetation phenology whilst reducing the effect of cloud contamination in the classification and interpretation of temporal signatures. The global scope of MODIS and the 13 years of available data to date is another strong justification for its use in national and regional level land cover mapping.

Smoothing and gap filling 8-day data could also be considered instead of MVC as a way to reduce cloud contamination and to increase the classification detail through better detection of key rice crop growth stages, but this would be more time consuming and require several further choices in terms of algorithms and thresholds. Our previous good experience with MVC was the basis for our decision to not use smoothing and gap filling. New sensors such as the RISAT-1 C band Synthetic Aperture Radar (SAR) sensor with 25 days repeat coverage in the same geometry, and multiband optical sensors such as PROBA-V and Sentinel-2 offer new possibilities for crop mapping with high temporal coverage, better spatial resolution and overcoming cloud effect in the case of SAR. Whether these new data sources can be used reliably with more automated mapping approaches remains to be seen.

The unsupervised classification of the NDVI time series provides a transparent approach to land cover mapping that can be reproduced and replicated in most situations. The challenge is to select a method which can identify rice classes from other classes consistently and with minimal subjective user interventions. A large set of field data that adequately samples the range of known cropping systems is one suitable way to relate the classes to observed land use and land cover. In this study, the distribution of field data points did not precisely follow the distribution of cropping systems, partially because of time and resource constraints but also because of gaps in knowledge of the cropping system locations. Indeed, if such precise information existed *a priori*, it would negate the need for studies like this!

Spectral matching and decision trees were used as operator guides for grouping similar classes. There will always be a degree of subjectivity in this grouping process, but extensive field information, local knowledge and ancillary information were all drawn upon to maximize the accuracy of the classification. Some areas of the country were not included in the field data campaign, partially due to time constraints, but also due to remoteness and flooding that limited access. We have provided the distribution of our ground truth points and suggest that remote sensing results in areas with little or no field data should naturally be treated with caution. Despite this, we observed that the spatial coverage was sufficient to allow most land cover classes to mapped with adequate accuracy in most cases and we believe the approach is a valuable contribution to rice mapping methodologies, especially in areas of high cropping intensity.

Field data collection is expensive, time consuming and challenging. There are several ways to reduce the burden including faster and less error prone field data capture using smart phones, the use of sensor webs and automated stations and crowd sourcing of voluntary geographic information to name a few. Still, field data collection can be the most expensive part of any remote sensing analysis and hence unsupervised and automated mapping approaches that do not rely heavily on field data have also been used to map rice areas over large geographic areas.

There is little dispute that rice mapping, as well as our knowledge of reflectance and vegetation indices over rice growing areas

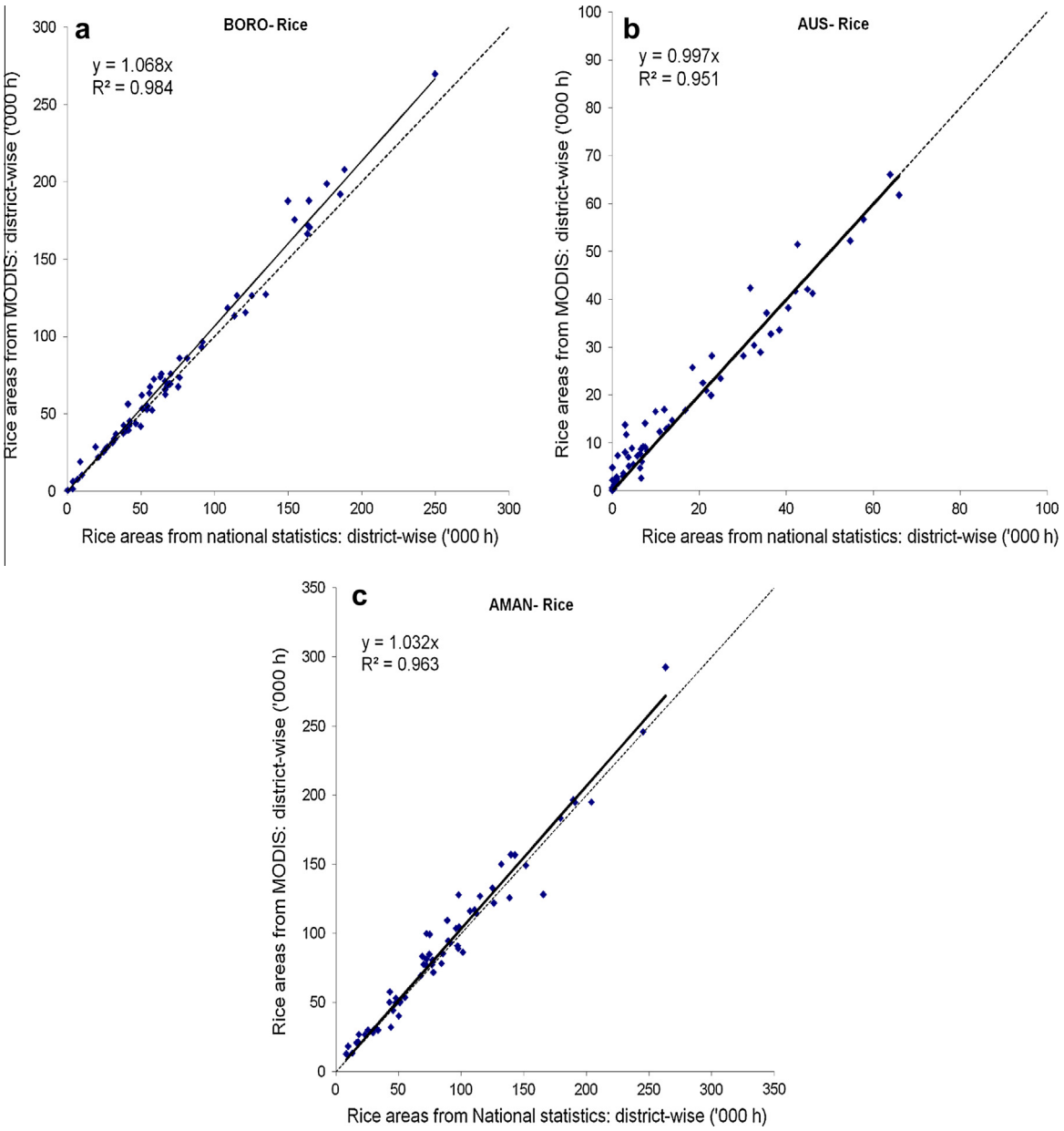

Fig. 7. District rice area by season from MODIS classification compared with national statistics (64 districts across study area) for (a) *boro*, (b) *aus*, and (c) *aman* rice.

would benefit from the generation of a library of temporal and spectral signatures that covered the wide range of environments and management practices of rice agriculture. The field data, MODIS signatures and local-knowledge-based interpretation in this paper are a contribution to such a library which would be a valuable global public good to refine, calibrate and validate both supervised and unsupervised approaches.

The field data were also used to address the low spatial resolution problem when data like MODIS are used to map and characterize ground features that are smaller than the pixel area and when multiple features occupy the same pixel. By generating sub pixel area estimates for each class we converted the MODIS pixel areas into rice class areas that were then compared to published rice area statistics. This sub pixel area approach depends on a field data set that fully captures the range of environments in which rice is cultivated.

The gaps in the field data and the challenges in collecting a comprehensive dataset are documented above. Further to this we need to add the subjective nature of the "eyeball" land cover proportion estimate that is conducted at each point. Despite these drawbacks, this approach is valid in the absence of cloud free high resolution imagery over the same number of environments and season. If only a small number of suitable high resolution images are available then the approach could be further validated by comparing the field operators land cover estimates to those from a land cover classification of the high resolution image (a general classification of crops, soil, water, forest and urban would suffice). If the areas are comparable then we can proceed with the percentage area estimates with greater confidence. Any discrepancies could be addressed by splitting the field data to account for cases where the sub pixel area of a class varies from one region to another. Naturally, if a greater number of high resolution scenes are available across the range of environments and seasons then the sub pixel area for each class could be computed directly without the need for field area estimates.

Getting the right area from the remote sensing data is one half of an equation that also depends on an independent and reliable source of area data with comparable spatial detail. If very high

resolution imagery or cadastral maps or field boundary data exist in sufficient quantities over the area then these can be used to estimate the accuracy of the moderate resolution classification (using sub pixel areas rather than pixel areas). Failing this, the most common approach is to use published statistical data from yearbooks, census' or other official sources. One major challenge here is that unless the statistical data rely on high resolution imagery as their main source of information then we will be comparing two very different ways of estimating area and this comparison may not be a fair one. For example, surveys may be based on a stratified sample of households and farm holdings extrapolated to give regional area estimates. These in turn rely on the accuracy of the farm level area estimates and the continuing validity of the stratification from year to year. In some cases the statistics are only published years after the event and the area estimates from previously published statistics may even be adjusted retroactively if the methodology is improved.

Furthermore, there are concerns in many countries that the statistics may be adjusted for political or other reasons such that they no longer reflect the original survey results. Evidence of this is hard to come by, often anecdotal and usually cannot be cited, but there are sufficient reports that make this issue impossible to ignore. In short, how can we be sure that the published statistics are reliable? If there is little information on their reliability how should we interpret any comparison between them and remotely sensed areas? This is not an easy issue to address and placing remote sensing as a better alternative to traditional area estimates ("our method is better than your method") may not be the most equitable resolution to the debate. One option could be to use remote sensing based area estimates and field campaigns to improve traditional estimates by identifying problem areas and adjusting the sampling or stratification accordingly. This backstopping of annual statistics could be the first step towards the acceptance of remote sensing as a valid tool in crop area estimation, particularly in emerging economies that contain much of the world's croplands. In the case of Bangladesh, we have no evidence to doubt the reliability of the published statistics and no other recourse.

5.3. Summary

This study applied unsupervised classification, spectral matching decision trees and supervised class labeling to map seasonal rice areas using hyper-temporal 500 m MODIS NDVI time-series data and intensive field-plot information. The accuracies of the rice area for each crop season [(*boro* (December/January–April), *aus* (April/May–June/July), and *aman* (July/August–November/December)] were determined by correlating the MODIS-derived sub-national (district-level) seasonal rice area statistics with the Bangladesh Bureau of Statistics sub-national statistics. The R^2 values were 0.96 for *boro* rice, 0.93 for *aus* rice, and 0.96 for *aman* rice. These statistical results also showed that the MODIS data overestimated rice area by 6% for *boro*, by 7% for *aus*, and by 3% for *aman* relative to the sub-national statistics. The overall accuracies of the five rice classes, during the three seasons, varied from 78% to 90%. However, rice versus non-rice accuracies exceeded 90%. Almost all intermixing was only between rice classes. The remote sensing based cropping intensity of rice determined in this study for Bangladesh was 149% across the country and was found to be 26% lower than previous non-remote sensing estimates.

Mapping seasonal rice areas is the first step in characterizing important rice-growing environments for sustainable development and livelihoods. Precise up-to-date seasonal rice maps and statistics such as these are important inputs for assessing the impact of abiotic stresses such as droughts and floods, which regularly affect the region and are predicted to increase in frequency and intensity in a changing climate. This approach was appropriate for accurate identification rice systems, rice cropping intensity and rice area estimates in most rice growing environments and seasons in Bangladesh. We documented the problem areas and discussed the possible shortcomings of the method as well as suggesting adjustments to the methodology in light of the findings of this study and forthcoming sensors. We suggest that this methodology can be improved and adapted for mapping rice in other countries where cropping intensity is high and where rice cultivation is extensive, including much of South, South East and East Asia where much of the world's rice is grown. The research makes a broad contribution to the methods and products of the Group on Earth Observations (GEO) for monitoring agriculture areas, Agriculture and Water Societal Beneficial Areas (GEO Agriculture and Water SBAs), the GEO Global Agricultural Monitoring Initiative (GEO GLAM), the global cropland area database using Earth observation data, and studies pertaining to global croplands, their water use, and food security in the 21st century.

Description

The spatial distribution of rice crop extent and area were derived for each of the three rice-growing seasons (*boro*, *aus*, and *aman*), in a 12-month period, of Bangladesh using MODIS 500 m 8-day time-series data, spectral matching techniques, decision tree algorithms, phenological approaches, and field-plot information.

Acknowledgments

This research was funded by the Bill & Melinda Gates Foundation projects "Stress-Tolerant Rice for Africa and South Asia" (STRASA) and "Green Super Rice" (GSR), and the Challenge Program on Water and Food (CPWF) Ganges Basin Development Challenge. The authors would like to thank Bill Hardy, science editor/publisher, IRRI, for editing this article. The authors thank Dr. Jauhar Ali, Dr. Abdel Ismail, Dr. Uma Shankar Singh, Mr. Arnel Rala, Dr. A. Bari, and Dr. Devendra Gauchan for their valuable feedback on early versions of the rice classification system. We would like to thank Prof. Daniel L. Civco, associate editor of this journal, and the three anonymous reviewers who helped in substantially improving the quality of this paper. The paper is not internally reviewed by the U.S. Geological Survey (USGS); hence, the opinions expressed here are those of the authors and not those of the USGS.

References

Allard, J., Kon, K., Morishima, Y., Kotzian, R., 2005. The crop protection industry's view on rice crop establishment in Asia and their impact on weed management techniques. In: Toriyama, K., Heong, K.L., Hardy, B. (Eds.), Rice is Life: Scientific Perspectives for the 21st Century. Proceedings of the World Rice Research Conference held in Tokyo and Tsukuba, Japan, 4–7 November, 2004. International Rice Research Institute, Los Baños, Philippines, and Japan International Research Center for Agricultural Sciences, Tsukuba, Japan, pp. 205–207.

Asaduzzaman, M., Ringler, C., Thurlow, J., Alam, S., 2010. Investing in crop agriculture in Bangladesh for higher growth and productivity, and adaption to climate change. Bangladesh Food Security Investment Forum, 26–27 May, 2010, Dhaka.

Badhwar, G.D., 1984. Automatic corn-soybean classification using landsat MSS data. I. Near-harvest crop proportion estimation. Remote Sens. Environ. 14, 15–29.

BBS, 2006. Bangladesh Bureau of Statistics and Ministry of Agriculture, The Government of the People's Republic of Bangladesh. Available at: <www.moa.gov.bd/statistics/bag.htm>. (accessed on 20.02.11).

BBS, 2010. Hand Book of Agriculture Statistics, Bangladesh Bureau of Statistics. <http://www.bbs.gov.bd/>. (accessed on 20.01.12).

BBS, 2011. Hand Book of Agriculture Statistics, Bangladesh Bureau of Statistics. <http://www.bbs.gov.bd/webtestapplication/userfiles/image/AgricultureCensus/>. (accessed on 20.01.12).

Biggs, T.W., Thenkabail, P.S., Gumma, M.K., Scott, C.A., Parthasaradhi, G.R., Turral, H.N., 2006. Irrigated area mapping in heterogeneous landscapes with MODIS time series, ground truth and census data, Krishna Basin, India. Int. J. Remote Sens. 27, 4245–4266.

Biradar, C.M., Thenkabail, P.S., Noojipady, P., Li, Y., Dheeravath, V., Turral, H., Velpuri, M., Gumma, M.K., Gangalakunta, O.R.P., Cai, X.L., Xiao, X., Schull, M.A., Alankara, R.D., Gunasinghe, S., Mohideen, S., 2009. A global map of rainfed cropland areas (GMRCA) at the end of last millennium using remote sensing. Int. J. Appl. Earth Obs. Geoinf. 11, 114–129.

Bouvet, A., Le Toan, T., 2011. Use of ENVISAT/ASAR wide-swath data for timely rice fields mapping in the Mekong River Delta. Remote Sens. Environ. 115, 1090–1101.

Cihlar, J., Xiao, Q., Beaubien, J., Fung, K., Latifovic, R., 1998. Classification by progressive generalization: a new automated methodology for remote sensing multichannel data. Int. J. Remote Sens. 19, 2685–2704.

Cohen, J.E., 2004. IV. Comparing Long-Range Global Population Projections With Historical Experience. World population to 2300. (<http://www.un.org/esa/population/publications/longrange2/WorldPop2300final.pdf>). (accessed on 15.07.12).

Dheeravath, V., Thenkabail, P.S., Chandrakantha, G., Noojipady, P., Reddy, G.P.O., Biradar, C.M., Gumma, M.K., Velpuri, M., 2010. Irrigated areas of India derived using MODIS 500 m time series for the years 2001–2003. ISPRS J. Photogramm. Remote Sens. 65, 42–59.

FAO, 2013. Arable Land (% Of Land Area), On-line Statistical Database of the Food and Agriculture Organization of the United Nations. Available on line <http://data.worldbank.org/indicator/AG.LND.ARBL.ZS>. (accessed on 21.01.13).

Frolking, S., Yeluripati, J.B., Douglas, E., 2006. New district-level maps of rice cropping in India: a foundation for scientific input into policy assessment. Field Crops Res. 98, 164–177.

Homayouni, S., Roux, M., 2003. Material Mapping from Hyperspectral Images using Spectral Matching in Urban Area. In: Landgrebe, P., (Ed.), IEEE Workshop in honour of Prof. Landgrebe, Washington DC, USA.

Gaur, A., Biggs, T.W., Gumma, M.K., Parthasaradhi, G.R., Turral, H., 2008. Water scarcity effects on equitable water distribution and land use in Major Irrigation Project – a case study in India. J. Irrig. Drain. Eng. 134 (1), 26–35.

Goetz, S.J., Varlyguin, D., Smith, A.J., Wright, R.K., Prince, S.D., Mazzacato, M.E., Tringe, J., Jantz, C., Melchoir, B., 2004. Application of multitemporal landsat data to map and monitor land cover and land use change in the Chesapeake Bay Watershed. In: Smits, P., Bruzzone, L. (Eds.), Analysis of Multi-temporal Remote Sensing Images. World Scientific Publishers, Singapore, pp. 223–232.

Gumma, M.K., Thenkabail, P.S., Muralikrishna, I.V., Velpuri, M.N., Gangadhararao, P.T., Dheeravath, V., Biradar, C.M., Acharya Nalan, S., Gaur, A., 2011a. Changes in agricultural cropland areas between a water-surplus year and a water-deficit year impacting food security, determined using MODIS 250 m time-series data and spectral matching techniques, in the Krishna River basin (India). Int. J. Remote Sens. 32, 3495–3520.

Gumma, M.K., Thenkabail, P.S., Nelson, A., 2011b. Mapping irrigated areas using MODIS 250 meter time-series data: a study on Krishna River Basin (India). Water 3, 113–131.

Idso, C.D., 2011. Estimates of Global Food Production in the Year 2050: Will We Produce Enough to Adequately Feed the World?, pp. 1–43. (<http://www.co2science.org/education/reports/foodsecurity/>). (accessed on 15.07.12).

Inoue, Y., Sakaiya, E., Zhu, Y., Takahashi, W., 2012. Diagnostic mapping of canopy nitrogen content in rice based on hyperspectral measurements. Remote Sens. Environ. 126, 210–221.

Islam, A.S., Bala, S.K., Haque, M.A., 2010. Flood inundation map of Bangladesh using MODIS time-series images. J. Flood Risk Manage. 3, 210–222.

Jensen, J.R., 2004. Introductory Digital Image Processing: A Remote Sensing Perspective, third ed. Prentice Hall, Upper Saddle River, NJ, p. 544.

Knight, J.F., Lunetta, R.L., Ediriwickrema, J., Khorram, S., 2006. Regional scale land-cover characterization using MODIS-NDVI 250 m multi-temporal imagery: a phenology based approach. GISci. Remote Sens. 43, 1–23.

Le Toan, T., Ribbes, F., Wang, L.-F., Floury, N., Ding, K.-H., Kong, J.A., Fujita, M., Kurosu, T., 1997. Rice crop mapping and monitoring using ERS-1 data based on experiment and modeling results. IEEE Trans. Geosci. Remote Sens. 35, 41–56.

Leica, 2010. ERDAS Field Guide, vol. 4, October 2010.

Lobell, D.B., Asner, G.P., Ortiz-Monasterio, J.I., Benning, T.L., 2003. Remote sensing of regional crop production in the Yaqui Valley, Mexico: estimates and uncertainties. Agric. Ecosyst. Environ. 94, 205–220.

Nguyen, T.T.H., De Bie, C., Ali, A., Smaling, E., Chu, T.H., 2012. Mapping the irrigated rice cropping patterns of the Mekong delta, Vietnam, through hyper-temporal SPOT NDVI image analysis. Int. J. Remote Sens. 33, 415–434.

Sakamoto, T., Yokozawa, M., Toritani, H., Shibayama, M., Ishitsuka, N., Ohno, H., 2005. A crop phenology detection method using time-series MODIS data. Remote Sens. Environ. 96, 366–374.

Shao, Y., Fan, X., Liu, H., Xiao, J., Ross, S., Brisco, B., Brown, R., Staples, G., 2001. Rice monitoring and production estimation using multitemporal RADARSAT. Remote Sens. Environ. 76, 310–325.

Thenkabail, P.S., 2010. Global croplands and their importance for water and food security in the twenty-first century: towards an ever green revolution that combines a second green revolution with a blue revolution. Remote Sens. 2, 2305–2312.

Thenkabail, P.S., Schull, M., Turral, H., 2005. Ganges and Indus river basin land use/land cover (LULC) and irrigated area mapping using continuous streams of MODIS data. Remote Sens. Environ. 95, 317–341.

Thenkabail, P.S., GangadharaRao, P., Biggs, T., Gumma, M.K., Turral, H., 2007. Spectral matching techniques to determine historical land use/land cover (LULC) and irrigated areas using time-series AVHRR pathfinder datasets in the Krishna River Basin, India. Photogramm. Eng. Remote Sens. 73, 1029–1040.

Thenkabail, P.S., Biradar, C.M., Noojipady, P., Dheeravath, V., Li, Y., Velpuri, M., Gumma, M., Gangalakunta, O.R.P., Turral, H., Cai, X., Vithanage, J., Schull, M.A., Dutta, R., 2009. Global irrigated area map (GIAM), derived from remote sensing, for the end of the last millennium. Int. J. Remote Sens. 30, 3679–3733.

Thiruvengadachari, S., Sakthivadivel, R., 1997. Satellite remote sensing for assessment of irrigation system performance: a case study in India. In: Research Report 9, International Irrigation Management Institute, Colombo, Sri Lanka.

Varlyguin, D., Wright, R., Goetz, S.J., Prince, S.D., 2001. Advances in land cover classification: a case study from the mid-Atlantic region. In: American Society for Photogrammetry and Remote Sensing, Proceedings, St. Louis, MO, p. 7. <http://www.geog.umd.edu/resac>.

Velpuri, N.M., Thenkabail, P.S., Gumma, M.K., Biradar, C.B., Noojipady, P., Dheeravath, V., Yuanjie, L., 2009. Influence of resolution in irrigated area mapping and area estimations. Photogramm. Eng. Remote Sens. 75, 1383–1395.

Vermote, E.F., Vermeulen, A., 1999. MODIS Algorithm Technical Background Document, Atmospheric Correction Algorithm: Spectral Reflectances (MOD09), NASA, Contract NAS5-96062.

WBP, 2012. Water Profile of Bangladesh, Food and Agriculture Organization. <http://www.eoearth.org/article/Water_profile_of_Bangladesh>. (accessed on 20.01.12).